atoms

MDPI

Article

Positron Impact Excitation of the 2*S* State of Atomic Hydrogen

A.K. Bhatia

Heliophysics Science Division, NASA/Goddard Space Flight Center, Greenbelt, MD 20771, USA; anand.k.bhatia@nasa.gov

Received: 17 May 2019; Accepted: 6 July 2019; Published: 10 July 2019

Abstract: The excitation cross-sections of the 2*S* state of atomic hydrogen at low (near threshold energy) to high incident positron energies (10.30 to 300 eV) have been calculated using the variational polarized-orbital method. Nine partial waves have been used to obtain converged cross-sections in the above energy range. The cross sections compared to the electron-impact excitation of the *S* state of atomic hydrogen are larger in the present case. The maximum cross section is 3.63(−1) πa_0^2 at 16.5 eV compared to 1.37(−1) πa_0^2 at 11.14 eV for the electron-impact excitation. The present results are compared with other calculations. Cross-sections have also been calculated in the Born approximation in which the polarization of the target has been included. Differential cross sections were calculated at k = 1.0 (13.6eV), 2.5 (85 eV), 3.483 (200 3V), and 4.696 (300 eV).

Keywords: positron-impact excitation

1. Introduction

Calculation of cross-sections for excitation of the 2*S* state of atomic hydrogen at low incident energies requires that coupled equations be solved. The close-coupling method has been applied by Burke et al. [1] in which the total wave function is expanded in eigenstates of the hydrogen atom to calculate the positron-impact excitation cross-sections of the 1*S* state to the 2*S* state of the atomic hydrogen. Their results are given in Table 1. The same method has been applied to calculate positron-impact excitation by Morgan [2]. The wave function has both 1*S* and 2*S* states, and therefore is equivalent to solving coupled equations. She used three-state and twelve-state bases obtaining 2.08(−1) and 2.61(−1) πa_0^2, respectively, for the excitation cross-section at k = 1.5. The present calculation gives 2.48(−1) πa_0^2 at k = 1.5, which is in good agreement with the cross section obtained by Morgan [2]. A close-coupled pseudostate approximation used by Walters [3] to calculate 1*S* to 2*S* and 2*P* excitation cross sections at four incident energies. His results are 1.27(−1), 6.1(−2), 3.0(−2), and 2.0(−2) πa_0^2 at 54.4, 100, 200, and 300 eV incident energies, respectively. His results are compared with the present results, given in Table 1. Calculations carried out by Kernoghan et al. [4], using a 33-state approximation between 0 and 110 eV incident energies. They used 1*s*, 2*s*, and 2*p* eigenstates of both positronium and hydrogen atoms, together with 27 hydrogen pseudostates, to calculate elastic scattering cross sections, H(2*s*) and H(2*p*) excitation cross sections. Their results are given in figures rather than in a numerical form, making it difficult to compare their results with the present results. However, some results have been extracted from their figure and are also given in Table 1. Calculations carried out by Das et al. [5] by applying a distorted wave theory that takes into account a polarization potential with a variable cutoff parameter and Lorentzian astrophysical plasma, for incident positron energies of 54.4, 100, and 200 eV, obtaining cross-sections of 1(−1), 5(−2), and 2(−2) πa_0^2, respectively, for 1*S* to 2*S* excitation. The calculations from this research gave 1.44(−1), 7.21(−2), 2.60(−2), and 1.28(−2) πa_0^2 at k = 2.0 (54.4 eV), 2.711 (100 eV), 3.843 (200 eV), and 4.696 (300 eV), respectively, which are fairly close to their results [5]. A close-coupling calculation has been carried out by Sarkar and Ghosh [6] with two basis sets of

hydrogen and positronium atoms. Calculations of excitation cross sections in the close-coupling approximation by Mitroy et al. [7] have been carried out using six hydrogenic and six positronium states. Their results are shown in Figure 8 of Reference [7]. They find excitation cross-sections increase in a linear manner as the incident energy is increased from the threshold to 1 Ry. Calculations have been carried out by Ratnavelu et al. [8] to obtain total cross-sections: elastic scattering, positronium formation, and ionization cross sections. Total cross-sections must include excitation to higher levels. However, they do not give any results for excitation cross-sections and estimating cross-sections for the 2*S* state only is unlikely. Moreover, their cross-sections have a 30% uncertainty. The present results are given in Table 1 and are compared with results obtained in References [1–6] wherever available.

Table 1. Present results (πa_0^2) for excitation of the 2*S* state of atomic hydrogen using the variational polarized orbital method with L_{max} = 8 and a comparison with the results obtained in references [1–6].

K	Present	Ref. [1]	Ref. [2]	Ref. [3]	Ref. [4]	Ref. [5]	Ref. [6]
0.87	9.35(−2)						
0.88	1.70(−1)						
0.90	2.47(−1)	5.9(−2)			3.25(−2)		
0.92	2.92(−1)						
0.95	3.32(−1)						
0.96	3.41(−1)						
1.00	3.61(−1)	1.46(−1)					
1.10	3.63(−1)	1.95(−1)					
1.20	3.38(−1)	2.13(−1)			1.38(−1)		
1.50	2.48(−1)	2.08(−1)	2.61(−1)				
1.60	2.20(−1)						
1.80	1.75(−1)			1.40(−1)			
2.00	1.44(−1)	1.38(−1)		1.27(−1)	1.25(−1)	9.90(−2)	
2.50	8.66(−2)						
2.711	7.21(−2)			6.10(−2)	7.00(−2)	5.70(−2)	5.80(−2)
3.843	2.60(−2)			3.00(−2)		3.00(−2)	2.90(−2)
4.4696	1.28(−2)			2.00(−2)			1.80(−2)

Electrons and positrons have the same mass. However, there is no exchange in the positron–atom interactions; therefore, the local interactions are not the same in the positron and electron interactions with the target. The effect of the polarization of the target is to produce an attractive long-range potential α_1/r^4, where α_1 is the polarizability of the target. This attractive potential is the same for positron and electron interactions with the atoms. The shift in energy due to the incident electron or positron at the hydrogen atom, in the dipole approximation, is of second order, and therefore it is proportional to the square of the electric field [9]. Therefore, the shift in energy does not depend on the direction of the electric field. Reversing the direction of the field does not have any effect. However, in the electron–atom interactions, the local and polarization potentials are both attractive and they add up to give a resultant attractive potential, while in the positron–atom interactions, the two potentials are of opposite sign and they tend to cancel each other.

Annihilation and positronium formation have been calculated earlier [10] and are not included in the present calculation because inclusion of both will give coupled equations. Moreover, annihilation takes place due to electromagnetic forces and is proportional to the cube of the fine structure constant, α. Clearly, it has to be treated separately. They have not even been included in the close-coupling calculations of Burke et al. [1], along with some other calculations, where it might have been easier. We use Ry units. Throughout, a(−b) implies a $\times 10^{-b}$.

The present calculation has been carried out using the variational polarized-orbital method [11]. The convergence of the present results is shown in Table 2. The present results are also shown in Figure 1, along with the results obtained by Burke et al. [1], Walters [3], and Kornoghan et al. [4]. Their

results are generally lower than the present results, except for the electron-impact excitation results of Burke et al. [1], which were higher except at a high energy; at high energy they are the same.

Table 2. Cross sections (πa_0^2) for 1*S* to 2*S* excitation in a variational polarized-orbital approximation.

k	$L_{max} = 0$	$L_{max} = 1$	$L_{max} = 2$	$L_{max} = 3$	$L_{max} = 4$	$L_{max} = 5$	$L_{max} = 6$	$L_{max} = 7$	$L_{max} = 8$
0.87	9.3473(−2)	9.3542(−2)	9.3542(−2)						
0.88	1.6913(−1)	1.6958(−1)	1.6958(−1)	1.6958(−1)					
0.90	2.4580(−1)	2.4574(−1)	2.4746(−1)	2.4747(−1)					
0.92	2.8914(−1)	2.2924(−1)	2.9244(−1)	2.9248(−1)	2.9248(−1)				
0.95	3.2599(−1)	3.3201(−1)	3.3204(−1)	3.3215(−1)	3.3217(−1)	3.3218(−1)	3.3218(−1)		
0.96	3.3363(−1)	3.4068(−1)	3.4072(−1)	3.4085(−1)	3.4089(−1)	3.4090(−1)	3.4090(−1)		
1.0	3.5002(−1)	3.6108(−1)	3.6109(−1)	3.6138(−1)	3.6150(−1)	3.6152(−1)	3.6153(−1)		
1.1	3.4147(−1)	3..6159(−1)	3.6168(−1)	3.6228(−1)	3.6278(−1)	3.6298(−1)	3.6304(−1)		
1.2	3.0884(−1)	3.3530(−1)	3.3602(−1)	3.3657(−1)	3.3747(−1)	3.3800(−1)	3.3819(−1)	3.3819(−1)	
1.5	2.0753(−1)	2.4031(−1)	2.4000(−1)	2.4520(−1)	2.4571(−1)	2.4589(−1)	2.4684(−1)	2.4743(−1)	2.4776(−1)
1.6	1.8106(−1)	2.1083(−1)	2.1166(−1)	2.1680(−1)	2.1720(−1)	2.1832(−1)	2.1963(−1)	2.1964(−1)	2.1964(−1)
1.8	1.3909(−1)	1.6455(−1)	1.7210(−1)	1.7306(−1)	1.7309(−1)	1.7369(−1)	1.7497(−1)	1.7502(−1)	1.7508(−1)
2.0	1.0830(−1)	1.2985(−1)	1.3853(−1)	1.4033(−1)	1.4048(−1)	1.40−64(1)	1.4135(−1)	1.4222(−1)	1.4302(−1)
2.5	6.1313(−2)	7.4516(−2)	8.0809(−2)	8.3483(−2)	8.6560(−2)	8.6596(−2)	8.6596(−2)	8.6596(−2)	8.6597(−2)
2.711	4.9474(−2)	6.0347(−2)	6.6592(−2)	6.8987(−2)	7.2110(−2)	7.2117(−2)	7.2119(−2)	7.2119(−2)	7.2119(−2)
3.834	1.8448(−2)	2.2409(−2)	2.4813(−2)	2.54458(−2)	2.5950(−2)	2.5957(−2)	2.5957(−2)	2.5958(−2)	2.5958(−2)
4.696	1.0044(−2)	1.2118(−2)	1.2505(−2)	1.2683(−2)	1.2809(−2)	1.2819(−2)	1.2821(−2)	1.2822(−2)	1.2822(−2)

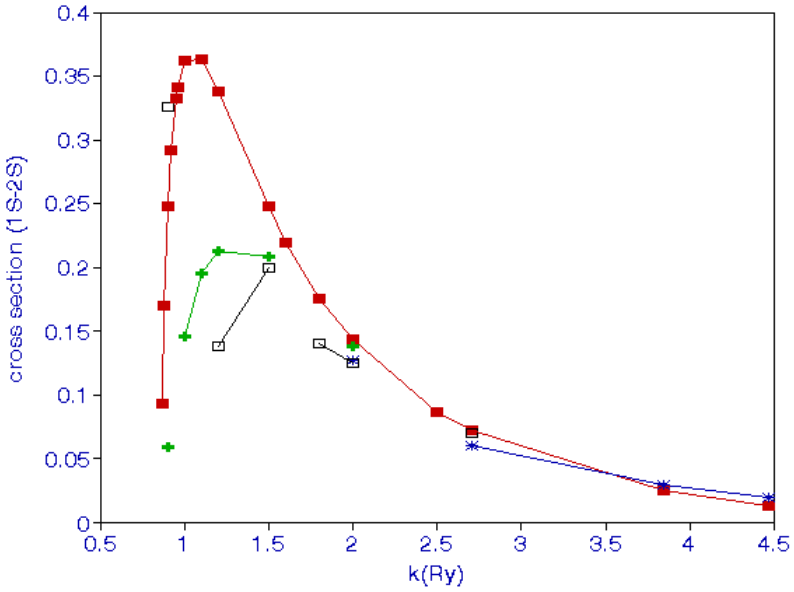

Figure 1. (Color online) Total 1*S*−2*S* excitation Cross Sections (πa_0^2) versus the incident momentum k (Ry). The green plus points represent the results of Burke et al. [1], the blue stars represent the results of Walters [3], and the black squares represent the results of Kernoghan et al. [4].

The maximum of these cross-sections is 3.63(−1) πa_0^2 at k = 1.1 (16.46 eV), and beyond this energy, cross-sections keep on decreasing with the increase of the incident energy, while the electron-impact excitation cross-sections of the atomic hydrogen have a maximum of 1.37(−1) πa_0^2 at 11.14 eV, then a minimum and another maximum [12]. This clearly indicates that the interactions with atoms for positrons and electrons are not the same.

2. Theory and Calculations

The present calculation has been carried out in the distorted-wave approximation. The total cross-section from a state "i" to a state "f" can be written in the form:

$$\sigma = \frac{k_f}{k_i}\int |T_{fi}|_2 d\Omega, \tag{1}$$

where k_i and k_f are the initial and final momenta and T_{fi} is a matrix element given by:

$$T_{fi} = -(\frac{1}{4\pi}) < \Psi_f|V|\Psi_i >, \tag{2}$$

In the above equation,

$$V = \frac{2Z}{r_1} - \frac{2}{r_{12}}; \tag{3}$$

$Z = 1$ is the nuclear charge; and the positions of the incident positron and target electron are given by r_1 and r_2, where $r_{12} = |\vec{r}_1 - \vec{r}_2|$. The nucleus is assumed to be of infinite mass. The incident wave function, which in principle, is an exact solution of the Schrödinger equation, is given by:

$$\Psi(\vec{r}_1, \vec{r}_2) = u(\vec{r}_1)\Phi^{pol}(\vec{r}_1, \vec{r}_2). \tag{4}$$

In order to include the polarization of the target, the effective target function can be written as:

$$\Phi^{pol} = \varphi_0(\vec{r}_2) + \frac{\chi(r_1)}{r_1^2}\frac{u_{1s\to p}(r_2)}{r_2}\frac{\cos(\theta_{12})}{\sqrt{Z\pi}}. \tag{5}$$

It should be noted that the second term has a plus sign rather than a negative sign, as in the case of electron scattering. $\phi_0(\vec{r}_2)$ is the target function. Temkin and Lamkin [13] have shown that the function $u_{1s\to p}$ is given by:

$$u_{1s\to p}(r_2) = e^{-Zr_2}(\frac{Z}{2}r_2^3 + r_2^2). \tag{6}$$

The term $\chi(r_1)/r_1^2 \to 0$ when $r_1 \to 0$. The cutoff function $\chi(r_1)$, introduced by Shertzer and Temkin [14], is given by:

$$\chi_{ST}(r_1) = 1 - e^{-2Zr_1}(\frac{1}{3}(Zr_1)^4 + \frac{4}{3}(Zr_1)^3 + 2(Zr_1)^2 + 2Zr_1 + 1). \tag{7}$$

This cutoff function was used only for the partial wave $L = 0$ and for higher partial waves to get more accurate wave functions, it was replaced by:

$$\chi(\beta r_1) = (1 - e^{-\beta r_1})^n, \tag{8}$$

where $n \geq 3$ [15]. This function gives us another nonlinear parameter β, which is a function of k, the incident positron momentum, along with the exponent n. Phase shifts were optimized to get an accurate scattering wave function. The scattering function $u(\vec{r}_1)$ in Equation (4) is given by:

$$u(\vec{r}_1) = a(L)\frac{u(r_1)}{r_1}Y_{Lo}(\Omega_1). \tag{9}$$

In the above equation, we have used the plane wave normalization:

$$a(L) = \sqrt{4\pi(2L+1)}. \tag{10}$$

$$u(r_1) = \frac{\sin(kr_1)}{kr_1} \; for \; r_1 \rightarrow \infty. \tag{11}$$

The equation for the scattering function is obtained from:

$$< Y_{L0}(\Omega_1)\Phi^{pol}(\vec{r}_1, \vec{r}_2)|H - E|\Psi_i(\vec{r}_1, \vec{r}_2) > . \tag{12}$$

The integration in the above equation is carried out over $d\Omega_1$ and $d\vec{r}_2$. The initial wave function is assumed to be exact and the final wave function, in the plane wave approximation, is given by:

$$\Psi_f = e^{i\vec{k}_f \cdot \vec{r}_1}\phi_{2S}(\vec{r}_2). \tag{13}$$

The excited state wave function is $\phi_{2S}(\vec{r}_2)$ and the cross section is given by:

$$\sigma(a_0^2) = \frac{k_f}{k_i}\int |T_{fi}|^2 P_L^2(\theta_{fi}) d\Omega_{fi}. \tag{14}$$

In the above equation, k_i and k_f are the initial and final momenta, and θ_{fi} is the angle between the initial and final states.

3. Cross-Sections

Cross-sections for excitation from the 1*S* to the 2*S* state have been calculated for the partial waves $L = 0$ to $L = 8$ and they are given Table 2 for various incident energies from $k_i = 0.87$ to 4.696. The convergence is good up to the fifth to sixth decimal places. The maximum cross-section is $3.63(-1)\pi a_0^2$ at $k_i = 1.1$ (16.46 eV). A comparison of the present results with the results of other calculations is given in Table 1.

If we replace $u(\vec{r}_1)$ in Equation (4) with $e^{i\vec{k}_i \cdot \vec{r}_1}$, we get the Born approximation. Cross-sections obtained in this approximation, shown in Table 3, are lower than those obtained in the present calculation.

Table 3. Cross-sections (πa_0^2) for 1*S* to 2*S* with a comparison of results obtained using the Born approximation and hybrid theory.

k	Born Approx.	Hybrid Theory
0.87	7.33(−2)	9.35(−3)
0.90	1.86(−1)	2.48(−2)
0.93	2.27(−1)	2.27(−1)
0.96	2.37(−1)	3.40(−1)
1.0	2.41(−1)	3.61(−1)
1.5	1.27(−1)	2.48(−1)
2.0	7.14(−2)	1.43(−1)
2.5	4.57(−2)	8.65(−2)
2.711	3.89(−2)	7.21(−2)
3.834	1.96(−2)	2.60(−2)
4.696	1.31(−2)	1.28(−2)

4. Differential Cross-Sections

The differential cross-section for excitation is given by:

$$\frac{d\sigma}{d\Omega} = \frac{k_f}{k_i}|\sum (2L+1)T_{fi}P_L(\cos\theta_{fi})|^2. \tag{15}$$

Differential cross-sections as a function of the scattering angles θ_{fi}, in an interval of 5°, are given in Table 4 for $k_i = 1.0$, 2.5, 3.834, and 4.696. Differential cross-sections at $k_i = 1.0$ increase from the value

at $\theta = 0°$ till $\theta = 60°$ and then start decreasing. Differential cross-sections at $k_i = 2.5$ has a maximum at 20° and keeps on decreasing till $\theta = 70°$, has another maximum at $\theta = 90°$, start decreasing again till $\theta = 150°$, and then start increasing again. Differential cross-sections at $k_i = 3.834$ and 4.696 had a maxima at $\theta = 0°$ and kept on decreasing with some oscillations toward the end. They are shown in Figure 2 for $k = 1.0$, and for other energies in Figure 3. In this figure, cross-sections are shown only up to $\theta = 60°$. Beyond this angle, they were getting close to zero. Walters [3] has calculated differential cross-sections at higher energies, but there is no indication of any structures, as shown in his figures [3].

Table 4. Differential cross sections (πa_0^2/degree), at k_i = 1.0, 2.5, and 3.834, and 4.696 at various scattering angles.

θ	$d\sigma/d\theta$			
θk	**1.0**	**2.5**	**3.834**	**4.696**
0	1.99(−2)	9.78	4.93	1.24
5	2.75(−2)	9.31	4.61	1.15
10	5.59(−2)	8.02	3.76	9.10(−1)
15	1.17(−1)	6.21	2.64	6.13−1)
20	2.20(−1)	4.28	1.55	3.49(−1)
25	3.57(−1)	2.57	7.21(−1)	1.67(−1)
30	5.08(−1)	1.29	2.33(−1)	6.83(−2)
35	6.40(−1)	4.95(−1)	3.33(−2)	2.53(−2)
40	7.27(−1)	1.10(−1)	7.22(−4)	1.03(−2)
45	7.52(−1)	1.55(−3)	1.92(−2)	5.91(−3)
50	7.18(−1)	2.60(−2)	2.60(−2)	5.04(−3)
55	6.42(−1)	7.20(−2)	1.35(−2)	4.87(−3)
60	5.44(−1)	8.29(−2)	9.91(−4)	4.21(−3)
65	4.44(−1)	5.48(−2)	3.95(−3)	2.94(−3)
70	3.55(−1)	1.66(−2)	1.969(−2)	1.68(−3)
75	2.82(−1)	2.15(−6)	3.33(−2)	9.08(−4)
80	2.24(−1)	1.63(−2)	3.25(−2)	6.76(−4)
85	1.79(−1)	5.04(−2)	1.84(−2)	8.76(−4)
90	1.44(−1)	7.53(−2)	3.52(−3)	1.49(−3)
95	1.15(−1)	7.33(−2)	9.89(−4)	2.33(−3)
100	9.07(−2)	4.78(−2)	1.36(−2)	2.88(−3)
105	7.02(−2)	1.74(−2)	3.16(−2)	2.61(−3)
110	5.35(−2)	8.60(−4)	4.02(−2)	1.57(−3)
115	4.07(−2)	4.84(−3)	3.20(−2)	4.35(−4)
120	3.16(−2)	2.24(−2)	1.32(−2)	3.88(−4)
125	2.57(−2)	4.03(−2)	4.48(−4)	6.10(−4)
130	2.22(−2)	4.78(−2)	7.07(−3)	1.89(−3)
135	2.04(−2)	4.10(−2)	3.19(−2)	3.07(−3)
140	1.95(−2)	2.36(−2)	5.78(−2)	3.42(−3)
145	1.86(−2)	5.43(−3)	6.45(−2)	2.69(−3)
150	1.74(−2)	1.14(−3)	4.48(−2)	1.30(−3)
155	1.54(−2)	2.64(−2)	1.40(−2)	1.52(−4)
160	1.30(−2)	9.12(−2)	1.14(−4)	2.63(−4)
165	1.05(−2)	1.92(−1)	2.32(−2)	2.08(−3)
170	8.39(−3)	3.06(−1)	7.83(−2)	5.09(−3)
175	7.05(−3)	3.97(−1)	1.35(−1)	7.91(−3)
180	6.59(−3)	4.32(−1)	1.60(−1)	9.06(−3)

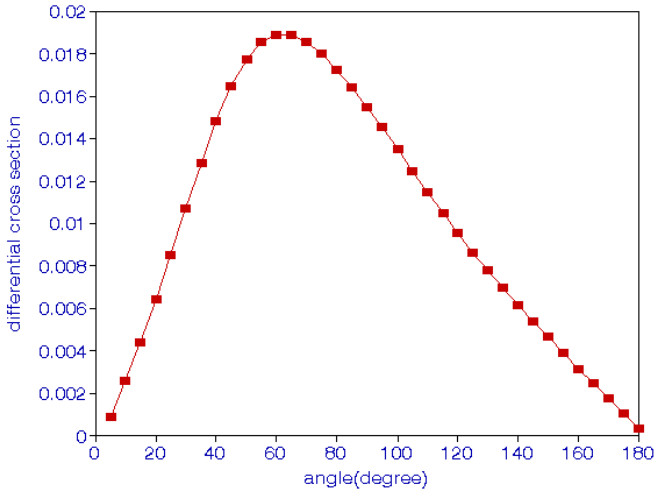

Figure 2. (Color online) Differential Cross Sections $(\pi a_0^2/\theta^\circ)$ versus angle θ at $k = 1.0$.

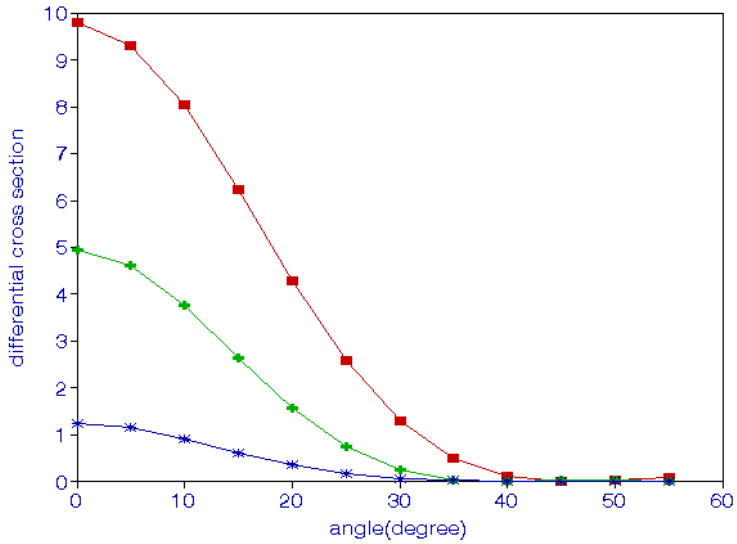

Figure 3. (Color online) Differential cross-sections $(\pi a_0^2/\theta^\circ)$ versus angle (°) at $k = 2.5$ (upper curve), 3.834 (middle curve), and 4.696 (lower curve).

5. Conclusions

Calculations for the excitation of the 2*S* state of the hydrogen atom from the 1*S* state were carried out in a distorted-wave approximation using the variational polarized-orbital method [15]. The phase shifts calculated in this approximation have lower bounds. This criterion has been used here to get accurate wave functions. At low incident energies, cross-sections were calculated at a fine energy interval. Using results between $k_i = 0.87$ (threshold) and 4.696 (200 eV), cross-sections at other k_i values can be obtained using interpolation. The present results have converged to at least five decimal places. Cross-sections have also been calculated in the Born approximation and they are lower than those obtained using the hybrid theory.

Positron impact excitation cross-sections were higher than those for electron-impact excitation cross-sections [12], as indicated in Figure 4. In a similar situation, proton-impact cross-sections were calculated by Saxena et al. [16], Cheshire and Sullivan [17], and Kolakowska et al. [18]. However, Sabbah and Tantawi [19] calculated cross-sections by proton impact as well as by antiproton impact. Their results are shown in Figure 2 of Reference [19] and they are seen to be of the same order, with the difference being that the proton impact cross-sections had a maximum at about 50 keV, just as in the present calculation, while the antiproton cross-sections decreased monotonically with the increase of

the incident energy. Figure 2 of Reference [19] is plotted using a log scale, and as such, it is very difficult to extract meaningful results. Whatever results could be extracted are given in Table 5. In the proton and antiproton excitation of the hydrogen atom, not only is there no exchange with the target electron, the masses are also different. The same is true when a muon and antimuon are used for excitation.

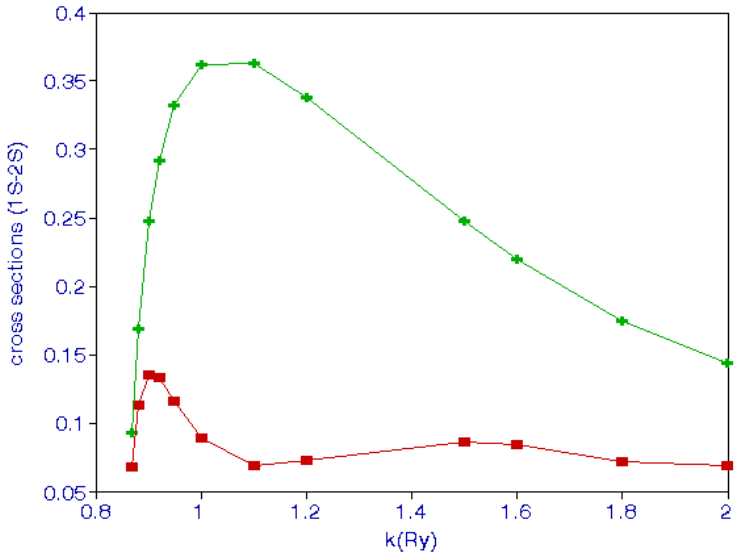

Figure 4. (Color online) Comparison of the excitation Cross Sections of positron (upper curve) and electron impacts (lower curve).

Table 5. Comparison of proton- and antiproton-impact excitation cross-sections (units are 10^{-17}cm^2).

E (keV)	Proton	Antiproton
6	0.5	0.8
10	2.5	4.0
20	5.0	3.0
60	2.0	0.8
100	0.8	0.5

Differential cross-sections were calculated at k_i = 1.0, 2.5, 3.834, and 4.696. There was no structure at low energies. However, there were maxima and minima at k = 2.5. Applications of the hybrid theory to calculate resonance parameters [20] and photoabsorption cross-sections [21] gave accurate results. Therefore, it is expected that the present excitation cross-sections are fairly accurate. The present results provide motivation for future experiments to measure excitation cross-sections and verify the calculated values. The experiments might also indicate the validity of methods and approximations used for calculations.

Funding: The research received no external funding.

Acknowledgments: Thanks are extended to R.J. Drachman and A. Temkin for helpful discussions. Calculations were carried out in quadruple precision using the Discover Computer at the NASA Center for Computation Science.

Conflicts of Interest: The author declares no conflict of interest.

References

1. Burke, P.G.; Schey, H.M.; Smith, K. Collisions of Slow Electrons and Positrons with Atomic Hydrogen. *Phys. Rev.* **1963**, *129*, 1258. [CrossRef]
2. Morgan, L.A. Positron impact excitation of the n=2 levels of hydrogen. *J. Phys. B At. Mol. Phys.* **1982**, *15*, L25–L29. [CrossRef]

3. Walters, H.R.J. Positron scattering by atomic hydrogen at intermediate energies: 1s-1s, 1s-2s, and 1s-2p transitions. *J. Phys. B At. Mol. Opt. Phys.* **1988**, *21*, 1893. [CrossRef]
4. Kernoghan, A.A.; Robinson, D.J.R.; McAlinden, M.T.; Walters, H.R.J. Positron scattering by atomic hydrogen. *J. Phys. B At. Mol. Opt. Phys.* **1996**, *29*, 2089–2102. [CrossRef]
5. Das, B.; Rej, P.; Kamali, M.Z.M.; Ghoshal, A. Positron Impact Excitation of Hydrogen Atom under Lorentzian Astrophysical Plasmas. *J. Fiz. Malays.* **2018**, *39*, 30001–30009.
6. Ghosh, A.S.; Sarkar, N.K. Positron-hydrogen scattering at low and medium energies using CCA. *J. Phys. B At. Mol. Opt. Phys.* **1994**, *27*, 759–779.
7. Mitroy, J.; Ratnavelu, K. The positron-hydrogen system at low energies. *J. Phys. B At. Mol. Opt. Phys.* **1995**, *28*, 287–306. [CrossRef]
8. Ratnavelu, K.; Brunger, M.J.; Buckman, S.J. Recommended Positron Scattering Cross Sections for Atomic Systems. *J. Phys. Chem. Ref. Data* **2019**, *48*, 023102. [CrossRef]
9. Merzbacher, E. *Quantum Mechanics*; John Wiley and Sons: New York, NY, USA; London, UK, 1998; p. 381.
10. Bhatia, A.K. P-Wave Positron-Hydrogen Scattering, Annihilation, and Positronium Formation. *Atoms* **2017**, *5*, 17. [CrossRef]
11. Bhatia, A.K. Hybrid theory of electron-hydrogen elastic scattering. *Phys. Rev. A* **2007**, *75*, 032713. [CrossRef]
12. Bhatia, A.K. Excitation of the 2*S* State of Atomic Hydrogen by Electron Impact. *Atoms* **2018**, *6*, 7. [CrossRef]
13. Temkin, A.; Lamkin, J.C. Application of the Method of Polarized Orbitals to the Scattering of Electrons from Hydrogen. *Phys. Rev.* **1961**, *121*, 788. [CrossRef]
14. Shertzer, J.; Temkin, A. Direct calculation of the scattering amplitude without partial-wave analysis. III. Inclusion of correlation effects. *Phys. Rev. A* **2006**, *74*, 052701. [CrossRef]
15. Bhatia, A.K. Hybrid theory of P -wave electron-hydrogen elastic scattering. *Phys. Rev. A* **2012**, *85*, 052708. [CrossRef]
16. Saxena, S.; Gupta, G.P.; Mathur, K.C. Excitation of the hydrogen atom from its ground and metastable states by positron and proton impact at intermediate energies. *J. Phys. B At. Mol. Phys.* **1984**, *17*, 3743. [CrossRef]
17. Cheshire, I.M.; Sullivan, E.C. *Excitation of Atomic Hydrogen by Proton*; NASA/Goddard Space Flight Center Publication: Greenbelt Rd, MD, USA, 1965.
18. Kołakowska, A.; Pindzola, M.S.; Robicheaux, F.; Schultz, D.R.; Wells, J.C. Excitation and charge transfer in proton-hydrogen collisions. *Phys. Rev. A* **1998**, *58*, 2872–2880. [CrossRef]
19. Sabbah, A.S.; Tantawi, R.S. Excitation of hydrogen atom by proton and antiproton. *Il Nuovo Cimento D* **1996**, *18*, 59–68. [CrossRef]
20. Bhatia, A.K. Applications of *P*-wave hybrid theory to the scattering of electrons from He^+ and resonances in He and H^-. *Phys. Rev. A* **2012**, *86*, 032709. [CrossRef]
21. Bhatia, A.K. Hybrid theory of *P*-wave electronLi^{2+} elastic scattering and photoabsorption in two-electron systems. *Phys. Rev. A* **2013**, *87*, 042705. [CrossRef]